

See discussions, stats, and author profiles for this publication at: <https://www.researchgate.net/publication/275823837>

# First-Principles Determination of the K-Conductivity Pathways in KAlO<sub>2</sub>

ARTICLE *in* THE JOURNAL OF PHYSICAL CHEMISTRY C · APRIL 2015

Impact Factor: 4.77 · DOI: 10.1021/acs.jpcc.5b01043

---

READS

19

2 AUTHORS, INCLUDING:



Maxim V Peskov

King Abdullah University of Science and Tec...

21 PUBLICATIONS 1,013 CITATIONS

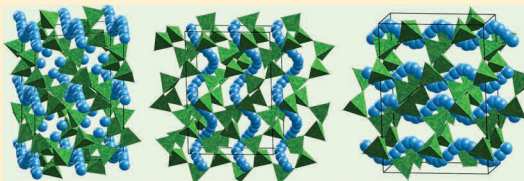
[SEE PROFILE](#)

# First-Principles Determination of the K-Conductivity Pathways in $\text{KAIO}_2$

Maxim V. Peskov and Udo Schwingenschlögl\*

Division of Physical Sciences and Engineering, King Abdullah University of Science and Technology, Thuwal 23955-6900, Kingdom of Saudi Arabia

**ABSTRACT:** Investigation of novel fast ion-conducting materials requires an accurate description of the ionic diffusion. The tiling method proposed by Blatov and coworkers, based on geometric characteristics, is a viable alternative to molecular dynamics simulations, allowing us to build models of the pathway system in crystal structures; however, the reliability is limited. Using first-principles simulations, we calculate the potential barriers of the ionic migration between voids in the structure of  $\text{KAIO}_2$  with local framework distortions and compare the results with those of the tiling method. We estimate the potential barriers for complex ion-conducting channels including several hopping distances. The effect of Coulomb interaction between charge carriers located in adjacent pathways on the potential barriers is discussed, and the effects of the framework flexibility are analyzed. Quantitative results on the potential barriers of ionic diffusion in a crystal structure and its dependence on the shape of the channels are important for assessing the potential of a specific compound.



## INTRODUCTION

Fast ion-conducting materials are indispensable for new-generation energy storage and power devices (supercapacitors and electrochemical and fuel cells). Among them, metal oxides with highly mobile  $\text{Li}^+$  and  $\text{Na}^+$  charge carriers, such as the lithium (LiSICON<sup>1</sup>) and sodium (NaSICON<sup>2</sup>) superionic conductors as well as olivine- and perovskite-type oxides, are frequently considered, but also compounds with larger cations (e.g.,  $\text{K}^+$ ) have gathered attention in recent years.<sup>3–6</sup> The description of the ion diffusion within a material is key for predicting its performance. In new compounds the ion-conducting pathways are not known and theoretical methods allowing us to predict them are rare.<sup>7–10</sup> In fact, the bulk of these approaches require assuming certain pathways and thus are limited to compounds of moderate complexity.<sup>7–9,11,12</sup> In this respect, general methods capable of discerning the ion-conducting channels, such as molecular dynamics simulations, are of great practical importance.

In many novel ion-conducting structures the computational effort to identify pathways is very high so that a method is required to initially generate a set of models for further validation by means of first-principles calculations or molecular dynamics. The tiling method proposed by Blatov and coworkers<sup>10</sup> is a viable alternative to molecular dynamics, making it possible to suggest models of the pathway system in crystal structures of any composition and complexity. Moreover, it facilitates pathway screening in potential ion conductors using large data sets extracted from structural databases, allowing us to avoid time-consuming simulations. The tiling method (and related to it the Voronoi–Dirichlet method) sees increasing use in materials chemistry for screening ion-conducting compounds.<sup>13–18</sup> One of the main disadvantages of the method is the full dependence on crystal structure features, namely, a set of predetermined empirical (ionic radii,

ion polarizability) and geometric (void volumes and sphericity, channel radii) parameters. Conclusions regarding the feasibility of pathways are derived based on such characteristics.<sup>17,18</sup> Because no framework relaxation is possible within this method, the purely geometric approach can lack reliability, as recently demonstrated by simulations using valence-bond force-fields.<sup>19</sup>

In the present work, we thus revise results of a recent application of the tiling method to the ion-conductor  $\text{KAIO}_2$ .<sup>20–22</sup> Using density functional theory, we calculate the potential barriers of ionic migration between voids and analyze its dependence on the shape and flexibility of the walls of ion-conducting channels. We focus on the energy barriers for  $\text{K}^+$  migration, that is, the effects of the strong interaction between  $\text{K}^+$  and the framework atoms on the mobility of the cations. The effects of Coulomb interaction between charge carriers located in adjacent pathways on the potential barriers are discussed. It is suggested that information about the energy barriers of the shortest (elementary) channels is sufficient to estimate the potential barriers along pathways running in arbitrary direction.

## COMPUTATIONAL DETAILS

The first-principles calculations were carried out with the VASP package using a plane-wave basis set in conjunction with projector augmented-wave pseudopotentials.<sup>23</sup> The electronic configurations  $3s^23p^1$  (Al),  $3s^23p^64s^2$  (K), and  $2s^22p^4$  (O) are considered in calculating the valence charge density. We use the Perdew–Burke–Ernzerhof functional,<sup>24</sup> a cutoff energy of 400

Received: February 1, 2015

Revised: April 4, 2015

Published: April 21, 2015

eV, and a  $\Gamma$ -centered Monkhorst–Pack grid<sup>25</sup> of  $10 \times 6 \times 4$  k-points to obtain fully converged structures and free energies. Optimization of the unit cell volume is achieved by a series of calculations with constant energy cutoff, followed by fitting of the obtained free energy values  $E(V)$  to the Birch–Murnaghan equation of state.<sup>26</sup> The following relaxation of the atomic positions employs the conjugated gradient algorithm. The final free energy is calculated for a fully optimized structure with atomic forces  $< 10^{-2}$  eV/Å. For constant-volume relaxation of the models with a fraction of the  $K^+$  ions displaced from the equilibrium positions to window centers, we relax the framework until the change in total energy between two structure steps is smaller than  $10^{-2}$  eV.

## STRUCTURAL MODELS

For building the structural models of  $KAlO_2$  the crystallographic data from ref 20 are used. The structure of the low-temperature modification of  $KAlO_2$  (space group  $Pbca$ ) contains two symmetry-inequivalent voids occupied by the cations  $K(1)$  and  $K(2)$ .  $KAlO_2$  has a diamond-type framework so that the voids are close to spherical. Each void is occupied by a  $K^+$  ion and shares faces with four other voids (Figure 1).

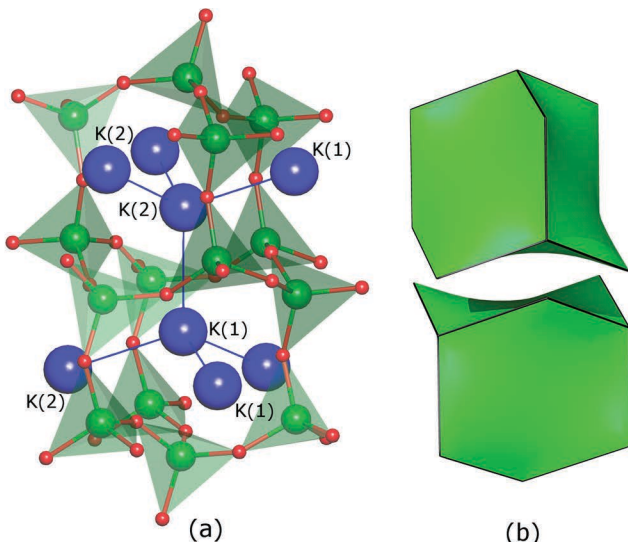


**Figure 1.** (a) Fragment of the structure of  $KAlO_2$  displaying two symmetry-inequivalent voids occupied by the cations  $K(1)$  and  $K(2)$ . The Al atoms are shown in green and the O atoms are shown in red. Each of the thin blue lines passes through a 12-membered ring shared by voids and is depicted to enhance the clarity of the Figure. (b) Two cages of the diamond structure.

According to natural tiling calculations,<sup>20</sup> five types of symmetry-inequivalent windows exist in the structure (Figure 2). The windows are formed by the O atoms of six corner-sharing  $[AlO_4]$  tetrahedra.

We give a brief description of the tiling model. The natural tiling for a crystal structure is a way of dividing the space into a set of minimal cages (tiles).<sup>27</sup> Tiles of the natural tiling have unambiguous physical meaning: The vertices are atoms and the edges are the interatomic bonds. Tiles are similar to polyhedra, but their faces may be nonplanar. Natural tiles enclose all voids of the structure with the faces forming windows that serve as gates between the voids. If a window is big enough, then small particles, such as ions, can pass through it. A window allowing ion migration is the bottleneck of the channel connecting two

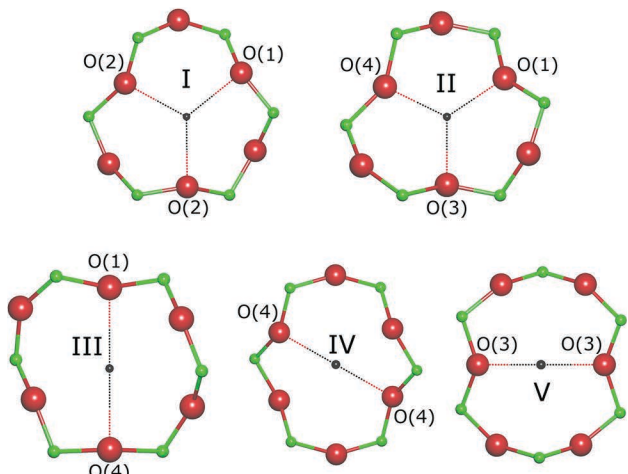


**Figure 2.** Five types of windows in the structure of the low-temperature modification of  $KAlO_2$  (tiling model). The Al atoms are shown in green and the O atoms are shown in red. The window centers are represented by black dots. The windows are nonplanar; that is, the O atoms of the window have an out-of-plane configuration.

particular voids. Any composite channel (further referred to as pathway) can be divided into a set of shortest segments connecting adjacent voids (see Figure 3), referred to as elementary channels in ref 20.

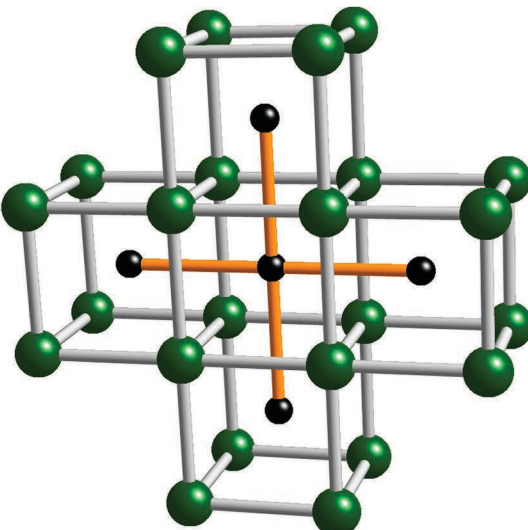


**Figure 3.** Fragment of the primitive cubic lattice consisting of five cube tiles. The black balls indicate the centers of the voids. Each tile shares four-membered rings with six other tiles. Elementary channels connecting adjacent voids are shown in orange. The composite channel connecting the left and right voids is the sum of two elementary channels meeting in the central void.

Because of the simplicity and high symmetry of the  $KAlO_2$  structure, the elementary channels are essentially linear, with a slight S-like bending in the channel–window crossing points. Therefore, finding the elementary channel bottlenecks does not require transition-state calculations, which routinely are done using the nudged elastic band method.<sup>9,28</sup>

Finding the lowest energy positions of  $K^+$  is achieved by relaxing the structure by the VASP code. They turn out to be the centers of the voids. In our simulations, we take into account the fact that any framework void can be occupied by

**Table 1.** Coordinates of the Centers of the Elementary Channel Bottlenecks in  $\text{KAlO}_2$ 

elementary channel	adjacent voids	nearest-neighbor O atoms			$r_{\min} (\text{\AA})^a$	window center		
		x	y	z		x	y	z
I	K(1), K(1)	O(2)	0.7992	0.1565	0.3514	2.436	0.5626	0.2677
		O(1)	0.5505	0.4853	0.2224			0.2459
		O(2)	0.2992	0.1565	0.1486			
II	K(1), K(2)	O(4)	0.0683	0.2848	0.4842	2.273	0.2672	0.3934
		O(3)	0.6782	0.4026	0.3940			0.3828
		O(1)	0.0505	0.4853	0.2776			
III	K(1), K(2)	O(1)	0.4495	-0.0147	0.2776	2.541	0.2411	0.6350
		O(4)	0.0683	0.2848	0.4842			0.3809
IV	K(2), K(2)	O(4)	0.9317	0.7152	0.5158	2.423	0	0.5
		O(4)	1.0683	0.2848	0.4842			0.5
V	K(2), K(2)	O(3)	0.3218	0.5974	0.6060	2.209	0.5	0.5
		O(3)	0.6782	0.4026	0.3940			0.5

<sup>a</sup>The minimal radius is the shortest distance between the center and the O atoms of the window.

**Table 2.** Equilibrium Volume of the  $\text{KAlO}_2$  Unit Cell

	$a (\text{\AA})$	$b (\text{\AA})$	$c (\text{\AA})$	volume ( $\text{\AA}^3$ )	method	space group
ref 20	5.4387	10.9236	15.4564	918.27	neutron diffraction experiment	<i>Pbca</i>
this work	5.5081	11.0630	15.6537	953.88	density functional theory	

one  $\text{K}^+$  ion only. Because all of the voids in the  $\text{KAlO}_2$  structure are occupied, modeling of the ionic movement along a selected pathway requires the simultaneous displacement of all of the cations in the pathway, as suggested by collective diffusion mechanisms. It allows us to maintain electroneutrality of the unit cell and to use in simulations the original cell. The symmetry of the structure is considered in the models; that is, we only analyze pathways built from inequivalent sets of elementary channels. To calculate the potential barrier for each pathway, we generate two models with the  $\text{K}^+$  ions occupying centers of the voids and centers of the windows (channel bottlenecks) of the pathway, respectively. The  $\text{K}^+$  positions in the channel bottlenecks are kept frozen. Coordinates of the window centers are calculated as midpoints of the segments connecting two nearest-neighbor nonbonded O atoms in opposite positions of the 12-ring for windows (III)–(V) and equidistant points of the three O atoms forming the channel bottlenecks for windows (I) and (II); see Table 1 and Figure 2. Calculation of the energies required for ions to hop between adjacent voids is straightforward. The potential barrier is defined by the energy difference between the transition state and the ground-state geometry.

## DISCUSSION

The interatomic distances (and hence potential barriers for mobile ions) are sensitive to structure details. Optimization of the  $\text{KAlO}_2$  unit cell (with the atomic positions fixed) gives a volume 3.9% larger than the experimental value reported in ref 20 (Table 2). Because of the systematic overestimation of lattice parameters by the generalized gradient approximation, the equilibrium volume should be slightly lower. Thus, we also investigate the changes in the potential barriers when the lattice constants are reduced by 1%, a value estimated to be the mean relative error for the Perdew–Burke–Ernzerhof functional.<sup>21</sup> The contraction of the unit cell is accompanied by a gain of 0.11 to 0.13 eV/ion in the potential barriers of the tiling model and a lower gain of 0.07 to 0.11 eV/ion in the barriers of the relaxed-framework model. Thus, we can expect that the

systematic error of the generalized gradient approximation does not undermine our conclusions.

We analyze the shortest pathways along the three unit cell vectors, that is, pathways without alternative paths and loops. Two kinds of pathways (1 and 2) along the [100] direction can be distinguished by the elementary channels they are built from, channel (I) (Figure 4a) and channels (IV) and (V) (Figure 4b).

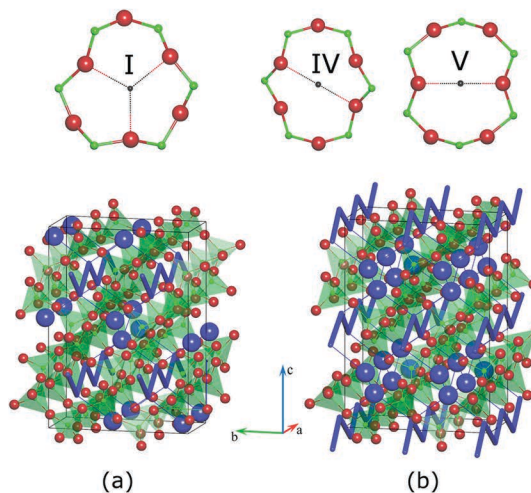


**Figure 4.** Ion-conducting pathways running along the  $a$  axis of the unit cell of  $\text{KAlO}_2$ . (a) Pathways 1 and (b) pathways 2 are built from the elementary channels (I) and (IV)+(V), respectively. By the simple channel trajectories, it follows that the centers of the windows are the transition states of the  $\text{K}^+$  diffusion between neighboring voids. Coordinates of the centers approximately correspond to those of the middle points of the thick blue lines.

Similarly, the [010] pathways (Figure 5), which also have a zigzag shape, are built from alternating elementary channels (II) and (III). The most complex geometry is realized for the helical pathways along the [001] direction. They consist of a combination of all five elementary channels of the low-temperature modification of  $\text{KAlO}_2$ ; see Figure 6. The

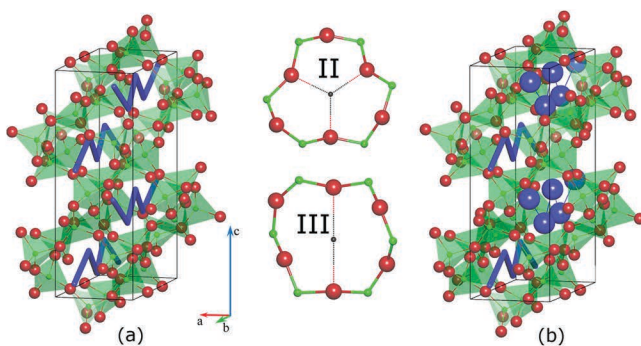


**Figure 5.** Ion-conducting pathways 3 running along the *b* axis of the unit cell of KAlO<sub>2</sub> with (a) four pathways in total and (b) only half of the pathways taken into account. The pathways are built from alternating elementary channels (II) and (III). By the simple channel trajectories, it follows that the centers of the windows are the transition states of the K<sup>+</sup> diffusion between neighboring voids. Coordinates of the centers approximately correspond to those of the middle points of the thick blue lines.

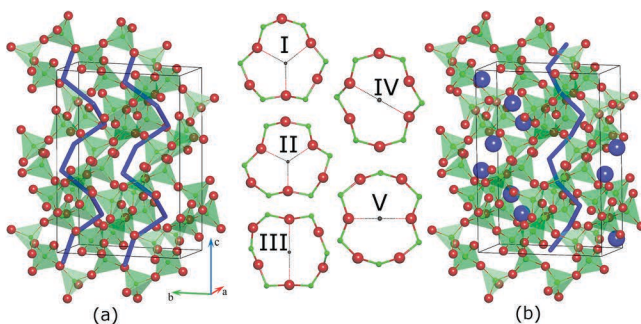


**Figure 6.** Helical ion-conducting pathways 4 running along the *c* axis of the unit cell of KAlO<sub>2</sub>. In (a) two pathways and in (b) only one pathway appear in the unit cell. The pathways are built from a combination of all five elementary channels. Window sequence in the pathways: [-(IV)-(II)-(I)-(II)-(V)-(III)-(I)-(III)-]<sub>n</sub>. Coordinates of the centers of the windows approximately correspond to those of the middle points of the thick blue lines.

following discussion consists of two parts. We undertake a critical review of the results obtained for the low-temperature modification of KAlO<sub>2</sub> using the tiling method in ref 20. This geometric approach makes predictions on the basis of experimental information about the atomic positions and does not consider structure relaxations. We will further refer

to this structural model with frozen framework positions as tiling model. Although the tiling model is a rather rough approximation, we use it to have a reference point for comparison of our results with those of Voronin and coworkers.<sup>20</sup> In the second part we address our calculations of the potential barriers in KAlO<sub>2</sub> with relaxed framework positions.

**Tiling Model.** We obtain moderate potential barriers for K<sup>+</sup> diffusion. When the framework atom positions are frozen, the potential barrier is 1.18 eV/ion for the helical pathways and marginally less (1.16 eV/ion) for diffusion along the *b* axis (Table 3, Figure 5). For diffusion along the pathways 1 and 2 (parallel to the *a* axis, see Figure 4), a considerable difference in the potential barrier is found ( $\Delta E = 0.18$  eV/ion), which is due to the corrugated shape of the windows (IV) included in pathway 2 and should hamper the conductivity. Using the tilings approach, it was suggested in ref 20 that KAlO<sub>2</sub> should possess a 2D conductivity. Our calculations, assuming unchanged framework positions, indicate that a 2D conductivity is unlikely; however, because the systems of pathways considered in this work and in ref 20 are different (the elementary channels (II) and (V) in ref 20 do not conduct), direct comparison is not possible.

Our results are consistent with the conclusions derived for KAlO<sub>2</sub> by the Voronoi–Dirichlet method in ref 22 with respect to the prediction of accessibility for K<sup>+</sup> only for pathway 1 and hence a 1D conductivity. The Voronoi–Dirichlet method maps voids using the vertices and edges of Voronoi polyhedra constructed for the framework atoms.<sup>10</sup> Although both the Voronoi–Dirichlet and tiling methods estimate the cross-section area of elementary channels to rule out those prohibiting ion migration, they employ different approaches to establish connectivity of the voids in a material.<sup>18,20</sup> This results in the prediction of lower dimensionality of the conductivity pathways in KAlO<sub>2</sub> by the former method.

A deformation of the outer electron shells of the K<sup>+</sup> ions is considered in ref 22 to be a factor steering the ionic diffusion by allowing K<sup>+</sup> to pass through the window openings with radii less than its ionic radius. Projections of the electron density of the 12-ring with K<sup>+</sup> in the center onto the ring plane show some elongation of the density around the O atoms of the ring in the direction of the Al–O bonds (Figure 7); however, no distortion of the charge density is seen around K<sup>+</sup>. Similarly, projections onto a plane orthogonal to the ring plane do not show any compression of the valence shells of the K<sup>+</sup> ions in

**Table 3. Potential Barriers for K<sup>+</sup> Migrating through Conductivity Pathways in KAlO<sub>2</sub>**

pathway	elementary channels	free energy (eV)		number of windows	potential barrier (eV/ion)	
		tiling model	relaxed-framework model		tiling model	relaxed-framework model
ground-state geometry				-400.43		
direction [100]						
pathway 1	(I)	-392.89	-394.59	8	0.94	0.73
pathway 2	(IV), (V)	-391.45	-395.08	8	1.12	0.67
pathway 1 + 2	(I), (IV), (V)	-382.84	-388.48	16	1.10	0.75
direction [010]						
pathway 3 (4 channels/unit cell)	(II), (III)	-381.84	-388.66	16	1.16	0.74
pathway 3 (2 channels/unit cell)	(II), (III)	-391.71	-394.79	8	1.09	0.71
direction [001]						
pathway 4 (2 channels/unit cell)	(I), (II), (III), (IV), (V)	-381.56	-387.10	16	1.18	0.83
pathway 4 (1 channel/unit cell)	(I), (II), (III), (IV), (V)	-391.24	-394.48	8	1.15	0.74

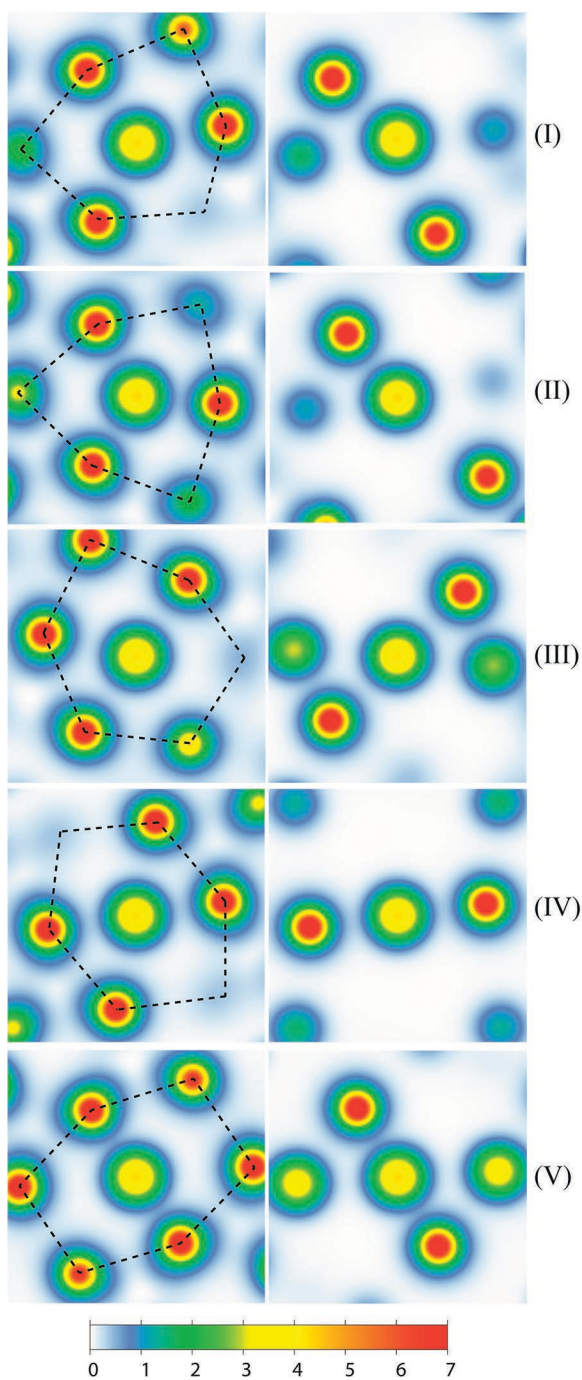


**Figure 7.** Maps of the electron density for five 12-ring windows with  $\text{K}^+$  occupying the window centers. Projections onto the window plane (right) and a plane orthogonal to it (left). Dashed lines indicate O atoms of the ring.

the window bottlenecks; see Figure 7. Therefore, we conclude that the deformation of the electron shells is negligible, having no effect on the ionic conductivity of  $\text{KAlO}_2$ .

**Relaxed-Framework Model.** Description of the framework atoms as static entities does not take into account local distortions when ionic diffusion takes place. Although atomic displacements are limited, the framework has some flexibility because the bond angles  $\text{O}-\text{Al}-\text{O}$  can change, manifesting itself in a slight variation of the window sizes and shapes. Indeed, our optimizations of the framework positions lead to a significant 22 to 40% decrease in the potential energy barriers,

which strongly influences the conductivity map. Pathway 1 shows a noticeably lower potential barrier, and an even more impressive reduction of the barrier height is found for pathway 2 because of a shape change of window (IV); see Figure 8.

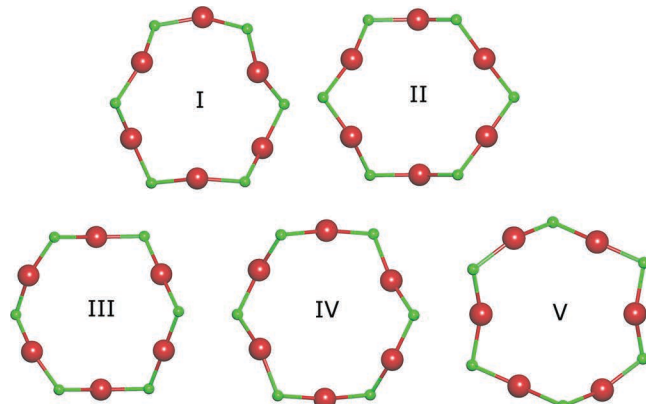


**Figure 8.** Five types of windows with  $\text{K}^+$  in the channel bottlenecks (relaxed-framework model) of the low-temperature modification of  $\text{KAlO}_2$ . The Al atoms are shown in green and the O atoms are shown in red.

According to Table 3, the potential barriers for  $\text{K}^+$  migration along the pathways 1, 2, and 3 become similar in energy under framework relaxation; that is, the framework adapts itself to lower the energies of transition states, which should enhance the transport. The potential barrier for pathway 4 (along the *c* axis) decreases less, maintaining a difference of 0.09 eV/ion with respect to the barriers of the pathways in the *ab* plane, for which we predict a smaller conductivity for the  $\text{K}^+$  ions; however, the potential barrier is not high enough to block the channel completely. Another reason for higher potential barriers along the *c* axis can be the strong K–K repulsion, as shown later. The limited  $\text{K}^+$  migration along the *c* axis explains the experimentally observed anisotropy of the conductivity in the low-temperature modification of  $\text{KAlO}_2$ .<sup>22</sup>

The potential barriers calculated for the pathways along the three unit cell axes allow us to estimate those associated with elementary channels. If a pathway is built of elementary channels of more than one type, the potential barriers of the individual channels cannot be calculated independently. At this point, we make an assumption that the channels (II) and (III) as well as (IV) and (V) have comparable barriers. This assumption is justified by the minimal radii ( $r_{\min}$ ) of the channels in the relaxed-framework model (Table 4). Therefore,

**Table 4. Potential Barriers for the Elementary Channels in the Relaxed-Framework Model**

channels	average potential barrier (eV)	$r_{\min}$ (Å)
(I)	0.73	2.706
(II) + (III)	0.74	2.744 and 2.737
(IV) + (V)	0.67	2.725 and 2.670

we average values over two or more types of elementary channels, that is, (II)+(III) and (IV)+(V); see Table 4. Note that this approach to calculate the potential barriers of the elementary channels cannot be used for the tiling model because of significant differences in the minimal radii (and hence the potential barriers) of the elementary channels (II) and (III) as well as (IV) and (V).

If the potential barriers for all elementary channels are known, they can be used for estimating the conductivity of a pathway along any arbitrary direction. For example, let us consider the 2D channel system studied in ref 20 that is built from the pathway 1 and composite channels consisting of two elementary channels (II) and one (IV) (Figure 9). If we assume

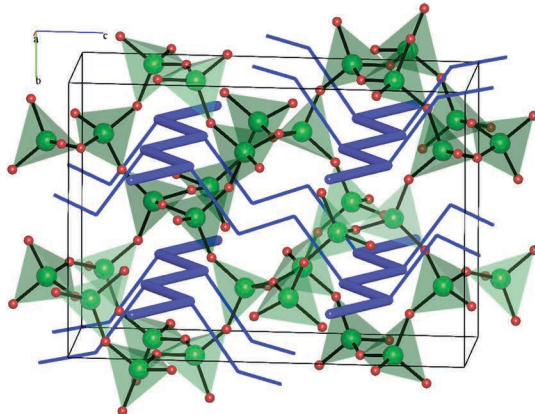


**Figure 9.** Two-dimensional channel system in the structure of  $\text{KAlO}_2$ , built of an array of pathways 1 (thick blue lines) connected by composite channels (thin blue lines) consisting of two elementary channels (II) and one (IV). The Al atoms are shown in green and the O atoms in maroon.

similar energies for the channels (II) and (III) as well as (IV) and (V) in the relaxed-framework model (Table 4), the potential barrier of the composite channel is determined by the highest barrier of the elementary channels included, that is, it is  $\text{Max}(0.67, 0.74) = 0.74 \text{ eV/ion}$ .

This estimate can slightly change because of interactions between cations residing in adjacent pathways. We evaluate this issue by calculating the potential barriers for half of the equally spaced pathways 3 and 4 (Figures 5 and 6, Table 3). Furthermore, we compare energies of the models with four and two pathways in the unit cell for pathways 3, and two and one pathway in the unit cell for pathways 4. These additional simulations clearly indicate interaction between cations, resulting in a large increase in the potential barrier for pathway 4 (+0.9 eV/ion). For the pathway 3 running along the  $b$  axis, the energy increase is three times lower (+0.3 eV/ion). The increased potential barriers are probably due to Coulomb forces between cations in proximity to each other as well as less framework response to the ionic diffusion, which points to slightly higher potential barriers in reality.

## CONCLUSIONS

We have calculated the potential barriers in the ion-conductor  $\text{KAlO}_2$  using density functional theory to validate probable ion-conducting pathways. We find that approaches not taking into account framework distortions can suffer from low accuracy, as reflected by wrong potential barriers. A significant drop in the potential barriers (up to 40%) is noticed as a result of the framework relaxation, accompanied by a widening of the channel bottlenecks, which is favorable for ion migration. Using a simple approach for simulating the ion migration in compounds with fully occupied voids, we have modeled local framework distortions as a result of ion movements and have estimated the potential barriers for infinite ion-conducting channels.

The potential barriers of the shortest symmetry-inequivalent (elementary) channels are found to determine the pathway characteristics. Therefore, knowledge of the elementary channel potential barriers makes it possible to establish the complete map of ion-conducting channels in a crystal structure. It would be beneficial for the criteria proposed in ref 18 for determining the ability of the elementary channels to conduct ions to include estimates of the potential barriers. Knowledge of the potential barriers associated with all elementary channels enables calculation of the potential barrier for diffusion through a channel of any complexity and length.

## AUTHOR INFORMATION

### Notes

The authors declare no competing financial interest.

## ACKNOWLEDGMENTS

Fruitful discussions with V. A. Blatov are gratefully acknowledged. Research reported in this publication was supported by the King Abdullah University of Science and Technology (KAUST).

## REFERENCES

- (1) Knauth, P. Inorganic Solid Li Ion Conductors: An Overview. *Solid State Ionics* **2009**, *180*, 911–916.
- (2) Anantharamulu, N.; Rao, K. K.; Rambabu, G.; Kumar, B. V.; Radha, V.; Vithal, M. A Wide-Ranging Review on Nasicon Type Materials. *J. Mater. Sci.* **2011**, *46*, 2821–2837.
- (3) Burmakin, E. I.; Voronin, V. I.; Akhtryanova, L. Z.; Berger, I. F.; Shekhtman, G. S. Potassium Aluminate Crystalline Structure and Electroconduction. *Russ. J. Electrochem.* **2004**, *40*, 619–625.
- (4) Kim, Y. W.; Oda, A.; Imanaka, N. Extraordinary High Potassium Ion Conducting Polycrystalline Solids Based on Gadolinium Oxide-Potassium Nitrite Solid Solution. *Electrochem. Commun.* **2003**, *5*, 94–97.
- (5) Kubel, F.; Fleig, J.; Pantazi, M.; Janushevsky, J. Ab-initio Structure Determination of the New Ion Conductor  $\text{K}_2\text{Al}_2\text{O}_3\text{F}_2$  from Powder Diffraction Data. *Z. Anorg. Allg. Chem.* **2011**, *637*, 41–45.
- (6) Trebala, M.; Bieniasz, W.; Holmlid, L.; Molenda, M.; Kotarba, A. Potassium Stabilization in  $\beta\text{-K}_2\text{Fe}_{22}\text{O}_{34}$  by Cr and Ce Doping Studied by Field Reversal Method. *Solid State Ionics* **2011**, *192*, 664–667.
- (7) Xu, L.; Wencong, L.; Chunrong, P.; Qiang, S.; Jin, G. Two Semi-Empirical Approaches for the Prediction of Oxide Ionic Conductivities in  $\text{ABO}_3$  Perovskites. *Comput. Mater. Sci.* **2009**, *46*, 860–868.
- (8) Wang, C.; Zhang, Q.-M.; Bernholc, J. Theory of Zn-Enhanced Disorder in GaAs/AlAs Superlattices. *Phys. Rev. Lett.* **1992**, *69*, 3789–3792.
- (9) Jalem, R.; Aoyama, T.; Nakayama, M.; Nogami, M. Multivariate Method-Assisted Ab Initio Study of Olivine-Type  $\text{LiMXO}_4$  (Main Group  $\text{M}^{2+}\text{-X}^{3+}$  and  $\text{M}^{3+}\text{-X}^{4+}$ ) Compositions as Potential Solid Electrolytes. *Chem. Mater.* **2012**, *24*, 1357–1364.
- (10) Blatov, V. A.; Shevchenko, A. P. Analysis of Voids in Crystal Structures: The Methods of 'Dual' Crystal Chemistry. *Acta Crystallogr., Sect. A* **2003**, *59*, 34–44.
- (11) Arrouvel, C.; Parker, S. C.; Islam, M. S. Lithium Insertion and Transport in the  $\text{TiO}_2\text{-B}$  Anode Material: A Computational Study. *Chem. Mater.* **2009**, *21*, 4778–4783.
- (12) Toyoura, K.; Koyama, Y.; Kuwabara, A.; Oba, F.; Tanaka, I. First-Principles Approach to Chemical Diffusion of Lithium Atoms in a Graphite Intercalation Compound. *Phys. Rev. B* **2008**, *78*, 214303.
- (13) Lupart, S.; Gregori, G.; Maier, J.; Schnick, W.  $\text{Li}_{14}\text{Ln}_5[\text{Si}_{11}\text{N}_{19}\text{O}_5]\text{O}_2\text{F}_2$  with  $\text{Ln} = \text{Ce, Nd}$  – Representatives of a Family of Potential Lithium Ion Conductors. *J. Am. Chem. Soc.* **2012**, *134*, 10132–10137.
- (14) Schneider, S. B.; Mangstl, M.; Friederichs, G. M.; Frankovsky, R.; auf der Gunne, J. S.; Schnick, W. Electronic and Ionic Conductivity

- in Alkaline Earth Diazenides  $\text{MAEN}_2$  ( $\text{M-AE} = \text{Ca, Sr, Ba}$ ) and in  $\text{Li}_2\text{N}_2$ . *Chem. Mater.* **2013**, *25*, 4149–4155.
- (15) Voronin, V. I.; Blatov, V. A.; Shekhtman, G. S. Specific Features of the Crystal Structure of Polymorphous Modifications of  $\text{KFeO}_2$  and Their Correlation with Ionic Conductivity. *Phys. Solid State* **2013**, *55*, 1050–1056.
- (16) Voronin, V. I.; Sherstobitova, E. A.; Blatov, V. A.; Shekhtman, G. Sh. Lithium-Cation Conductivity and Crystal Structure of Lithium Diphosphate. *J. Solid State Chem.* **2014**, *211*, 170–175.
- (17) Anurova, N. A.; Blatov, V. A.; Ilyushin, G. D.; Blatova, O. A.; Ivanov-Schitz, A. K.; Dem'yanets, L. N. Migration Maps of  $\text{Li}^+$  Cations in Oxygen-Containing Compounds. *Solid State Ionics* **2008**, *179*, 2248–2254.
- (18) Blatov, V. A.; Ilyushin, G. D.; Blatova, O. A.; Anurova, N. A.; Ivanov-Schitz, A. K.; Dem'yanets, L. N. Analysis of Migration Paths in Fast-Ion Conductors with Voronoi–Dirichlet Partition. *Acta Crystallogr., Sect. B* **2006**, *62*, 1010–1018.
- (19) Adams, S.; Rao, R. P. High Power Lithium Ion Battery Materials by Computational Design. *Phys. Status Solidi A* **2011**, *208*, 1746–1753.
- (20) Voronin, V. I.; Shekhtman, G. S.; Blatov, V. A. The Natural Tiling Approach to Cation Conductivity in  $\text{KAlO}_2$  Polymorphs. *Acta Crystallogr., Sect. B* **2012**, *68*, 356–363.
- (21) Haas, P.; Tran, F.; Blaha, P. Calculation of the Lattice Constant of Solids With Semilocal Functionals. *Phys. Rev. B* **2009**, *79*, 085104.
- (22) Voronin, V. I.; Surkova, M. G.; Shekhtman, G. S.; Anurova, N. A.; Blatov, V. A. Conduction Mechanism in the Low-Temperature Phase of  $\text{KAlO}_2$ . *Inorg. Mater.* **2010**, *46*, 1234–1241.
- (23) Kresse, G.; Joubert, D. From Ultrasoft Pseudopotentials to the Projector Augmented-Wave Method. *Phys. Rev. B* **1999**, *59*, 1758–1775.
- (24) Perdew, J. P.; Burke, K.; Ernzerhof, M. Generalized Gradient Approximation Made Simple. *Phys. Rev. Lett.* **1996**, *77*, 3865–3868.
- (25) Monkhorst, H. J.; Pack, J. D. Special Points for Brillouin-Zone Integrations. *Phys. Rev. B* **1976**, *13*, 5188–5192.
- (26) Birch, F. Finite Elastic Strain of Cubic Crystals. *Phys. Rev.* **1947**, *71*, 809–824.
- (27) Blatov, V. A.; Delgado-Friedrichs, O.; O'Keeffe, M.; Proserpio, D. M. Three-Periodic Nets and Tilings: Natural Tilings for Nets. *Acta Crystallogr., Sect. A* **2007**, *63*, 418–425.
- (28) Kendrick, E.; Kendrick, J.; Knight, K. S.; Islam, M. S.; Slater, P. R. Cooperative Mechanisms of Fast-Ion Conduction in Gallium-Based Oxides with Tetrahedral Moieties. *Nat. Mater.* **2007**, *6*, 871–875.